This article has been accepted for publication in a future issue of this journal, but has not been fully edited. Content may change prior to final publication. Citation information: DOI 10.1109/JQE.2017.2704929, IEEE Journal of Quantum Electronics

Image-free Microwave Photonic Down-Conversion Approach for Fiber-Optic Antenna Remoting

Peixuan Li, Wei Pan, Xihua Zou, *Senior Member, IEEE*, Bing Lu, Lianshan Yan, *Senior Member, IEEE*, and Bin Luo

***Abstract*—For commercial and military applications, it is highly desired to acquire broadband radio frequency (RF) signals from remotely located receiving antennas to the central office (CO) for centralized signal processing such as down-conversion. In this paper, a photonic approach for image-free microwave frequency down-conversion is proposed for antenna remoting scenarios. The RF signal is captured by the phase modulator (PM) at remote antenna unit and transmitted over a long fiber link to the CO for performing frequency down-conversion. In analog with the Hartley architecture in the electronic domain, two in-phase (I) and quadrature (Q) intermediate frequency (IF) components are generated by using an electro-optic polarization modulator (PolM) and two polarizers. To achieve large image rejection ratio (IRR), the digital post-processing technique is introduced to accurately compensate the amplitude and phase imbalances between the I and Q IF signals. In the experiments, a 2-km single-mode fiber link is inserted between the PM and PolM. As the LO signals are set as 35 GHz and 3 GHz, two target sinusoidal signals at 35.5 and 3.1 GHz are applied with two image signals, a sinusoidal signal at 34.5 GHz and a broadband RF signal centered at 2.9 GHz, respectively. Then both real-time analog and off-line digital processing methods are used to process the generated I and Q IF signals for image rejection, yielding an IRR over 45 and 60 dB respectively, when the sinusoidal image signal is applied. The distortions from the broadband 2.9-GHz image RF signal is also effectively suppressed by using the two processing methods. The proposed approach is capable of covering a wide frequency range from 5 to 40 GHz.**

***Index Terms*—microwave photonics, antenna remoting, photonic frequency down-conversion, image reject, digital signal processing.**

I. Introduction

MICROWAVE frequency down-conversion is of critical importance in the microwave systems. Compared with the down-conversion implemented by conventional electrical mixer, the microwave photonic mixer (MPM) is characterized by high isolation, low transmission loss, wide bandwidth, and immunity to the electromagnetic interference. In addition, assisted by long fiber-optic links, the frequency down-conversion using MPM has been considered as an enabling solution to meet the demand of antenna remoting applications, such as radio over fiber (RoF), cellular wireless network, electronic warfare, remote sensing and radar [1]-[4].

Regarding MPMs, cascaded electro-optic modulators (EOMs) [5], [6] are frequently used, providing high isolation between radio frequency (RF) signal port and microwave local oscillator (LO) signal port within a wide operation bandwidth. Subsequently, a number of distinct MPMs have been proposed [7]-[16] to improve the key performance indicators, including conversion efficiency [7], [8], spurious free dynamic range (SFDR) [9]-[15], idle frequency suppression [16]. Nevertheless, the MPM is usually implemented through a heterodyne structure to obtain a nonzero intermediate frequency (IF) signal, while an existing image signal might bring in-band interferences. The target signal and image signal, which are located at both sides of the LO signal with approximately equal frequency spacing, will be translated to the same IF band. Although the image signal can be filtered out prior to down-conversion [17], it is arduous to build filter with sufficient selectivity and high dynamic range for high-frequency RF signals and low-frequency IF signals. Another practical alternative architecture can be the Weaver and Hartley architectures, where the image signal can be effectively suppressed using in-phase (I) and quadrature (Q) conversion systems without filter [18]. In recent years, a few MPMs using Hartley architecture have been reported to solve the problem of image [19]-[22]. In [19], an electrical LO 90-degree hybrid is needed and only the numerical simulation is performed. The 90-degree optical hybrid and microwave photonic phase shifter are introduced in [20]-[22] to obtain I and Q IF signals and an image rejection ratio (IRR) of ~60 dB is observed in the experiments. In addition, in [23], an integrated dual-parallel Mach–Zehnder modulator (MZM) with a 90-degree polarization rotator in one arm is used to achieve high conversion efficiency and image rejection.

The frequency down-conversion approaches in [20]-[23] might be proposed for local scenarios, where LO signal synthesizer with filtering or bias control should be assembled in the same receiving unit. While for antenna remoting scenarios where RF signal receiving at remote location from the base station in RoF or electronic warfare systems, simplified receiving unit is more desired. A typical antenna remoting or fiber-based microwave signal relay scenario can be seen in [24], demonstrating the cloud-ROF access scheme. In the

Manuscript received, 2016. This work was supported in part by the National "863" Project of China under grant 2015AA016903 and by the National Natural Science Foundation of China under grants 61372061 and 61378008.

P. Li, W. Pan, X. Zou, B Lu, L. Yan, B, Luo are with the Center for Information Photonics and Communications, School of Information Science and Technology, Southwest Jiaotong University, Chengdu 610031, China (zouxihua@swjtu.edu.cn).

This article has been accepted for publication in a future issue of this journal, but has not been fully edited. Content may change prior to final publication. Citation information: DOI 10.1109/JQE.2017.2704929, IEEE Journal of Quantum Electronics

cloud-ROF access system, only optic-electro/electro-optic conversion, and RF antennas are needed at the remote antenna unit (RAU), while digital-to-analog/analog-to-digital conversion and RF frontend functions should be shifted to the baseband processing unit (BBU), i.e., central office (CO). This centralized signal processing can enable more advanced and efficient network coordination and management. Accordingly, for some applications involving antenna remoting, the RF port and LO port locating at different unit is more preferable. A microwave photonic down-conversion approach that uses cascaded phase modulators is proposed in [25], which can find applications in heterodyne image rejection and fiber-optic antenna remoting. However, the need of an electrical LO 90-degree hybrid and three modulators makes the system complicated. Furthermore, the MPMs with Hartley architecture will suffer from the problem of imbalances of phase and amplitude between two signal paths, and the IRR is limited to around 30–40 dB for 1°–5° phase imbalance or 0.2–0.6 dB amplitude imbalance [18]. Hence, we proposed a microwave down-conversion approach with large IRR utilizing digital signal processing in [26], where the digital post-processing method is used to accurately compensate for the amplitude and phase imbalances between the I and Q IF signals.

In this paper, we describe in detail this photonic microwave frequency down-conversion approach with image rejection for antenna remoting. In the proposed scheme, the RAU and CO are connected by optical fiber link for transmission of RF signal over a long distance. When the deployment and maintenance costs are taken into account, the simplified RAU consists of a bias-free phase modulator to facilitate electro-optic modulation. At the CO, the phase-modulated optical signal is remodulated by an LO signal through the polarization modulator (PolM). The PolM is incorporated with optical bandpass filter (OF) and polarizers to generate I and Q IF signals. Furthermore, since the low-frequency IF signals can relax the requirement of sample rate of analog-to-digital converter (ADC) and the improvement of SFDR of MPM using digital post-processing have been intensively studied in the past few years [10]-[13]. In this paper, the digital post-processing technique is used to accurately compensate for the amplitude and phase imbalances between two generated I and Q IF signals for large IRR. In the proof-of-concept experiments, after transmission over a 2-km fiber link, the target sinusoidal signals at 35.5 GHz is successfully down-converted to a 0.5-GHz IF signal. When applying an image sinusoidal signal at 34.5 GHz, the real-time analog processing and off-line digital processing of generated I and Q IF signals for image rejection are carried out, respectively. An IRR over 45 dB or 60 dB is achieved for the real-time processing or off-line processing. As another case, a target sinusoidal signal at 3.1 GHz is down-converted to a 0.1-GHz IF signal with effective suppression of distortion from a broadband image RF signal carrying baseband data and centering at 2.9 GHz. Furthermore, the RF signals ranging from 5 to 40 GHz are successfully down-converted to the 500-MHz IF signals.

II. Principle

A. Hartley architecture for image rejection

The Hartley image-reject architecture is shown in Fig. 1. The input RF signal is firstly mixed with the quadrature outputs of LO signal and filtered by the low pass filters to generate I and Q IF signals. Afterwards, the signal at one of the two paths will experience a 90° phase shift before adding them together. As the principle illustrated in Fig. 1, the IF signals at two paths contain the target signal with same polarity and the image signal with opposite polarity. Therefore, the image signal is canceled through the summation of signals from two paths, while the target signal is maintained [18].

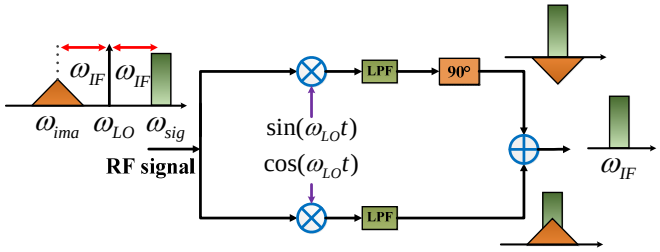

Fig.1. Hartley architecture for image rejection. LPF: low pass filter.

B. Photonic generation of I and Q IF signals

Inspired from the Hartley image-reject architecture presented above, the schematic diagram of the proposed microwave photonic down-conversion approach is shown in Fig. 2(a). The target and image RF signals are received by the antenna at RAU. The optical carrier from a laser source is modulated by the received RF signals through PM. When the target and image RF signals with angular frequencies at $\omega_{RF} = \omega_{LO} \pm \omega_{IF}$ are applied to the RF port of PM, the output electrical field of PM can be expressed as

$$E_{PM}(t) \propto E_{in} e^{j\omega_c t} e^{j\beta_1 \cos(\omega_{RF} t)}, \quad (1)$$

where E_{in} and ω_c are the amplitude and angular frequency of optical carrier, $\beta_1 = \pi \cdot (V_{RF} / V_{\pi 1})$ is the modulation index of PM, which is related to the amplitude of input RF signals (i.e., V_{RF}), $V_{\pi 1}$ is the half-wave voltage of PM. Then, the phase modulated lightwave is sent to the CO through fiber link. Under small signal modulation, the electrical field of the phase-modulated lightwave after the transmission over a segment of fiber link is expressed as

$$E_{PMF}(t) \propto E_{in} e^{j\omega_c t} \left(J_{01} e^{j\theta_0} + jJ_{11} e^{j(\omega_{RF} t + \theta_1)} + jJ_{11} e^{-j(\omega_{RF} t - \theta_2)} \right), \quad (2)$$

where $J_{kr} = J_k(\beta_r)$ and $J_n(\cdot)$ is the nth-order Bessel function of first kind. θ_i ($i = 0,1,2$) are the additional phases introduced by the fiber link. At the CO, the phase-modulated lightwave is injected into the PolM, oriented at an angle of 45° to one principle axis of PolM. Since the PolM is a special phase modulator that supports both transverse-electric (TE) and transverse-magnetic (TM) modes with opposite phase modulation indices. LO signal with angular frequency ω_{LO} is applied to the PolM and the output electrical fields of two

This article has been accepted for publication in a future issue of this journal, but has not been fully edited. Content may change prior to final publication. Citation information: DOI 10.1109/JQE.2017.2704929, IEEE Journal of Quantum Electronics

orthogonal directions of PolM can be written as

$$\begin{bmatrix} E_x \\ E_y \end{bmatrix} \propto E_{PMF}(t) \begin{bmatrix} e^{j\beta_2 \cos(\omega_{LO} t)} \\ e^{-j\beta_2 \cos(\omega_{LO} t)} \end{bmatrix}, \quad (3)$$

in which $\beta_2 = \pi \cdot (V_{LO} / V_{\pi 2})$ is the modulation index of PolM, which is related to the amplitude of input LO signal (i.e., V_{LO}), $V_{\pi 2}$ is the half-wave voltage of PolM. Afterwards, to implement a microwave photonic phase shifter (MPS) for the IF signals, the remodulated optical wave is sent to an OF to eliminate the lower sidebands, yielding a single sideband modulation (SSB) [27]. Under small signal modulation condition, the output of OF can be written as

$$\begin{bmatrix} E_x \\ E_y \end{bmatrix} \propto E_{in} e^{j\omega_c t} \begin{bmatrix} J_{01}J_{02}e^{j\theta_0} + jJ_{02}J_{11}e^{j(\omega_{RF}t+\theta_1)} + jJ_{01}J_{12}e^{j(\omega_{LO}t+\theta_0)} \\ J_{01}J_{02}e^{j\theta_0} + jJ_{02}J_{11}e^{j(\omega_{RF}t+\theta_1)} - jJ_{01}J_{12}e^{j(\omega_{LO}t+\theta_0)} \end{bmatrix}, \quad (4)$$

The filtered optical signal is then amplified by the Erbium-doped fiber amplifier (EDFA) and split into two paths by a 3-dB optical coupler, where each path contains a polarization controller (PC) and a polarizer. At one path, by adjusting the PC before polarizer, the polarization direction of polarizer is oriented at an angle of α to one principal axis of the PolM. The combined electrical field at the output of the polarizer is

$$E_{Pol}(t) \propto \cos\alpha E_x + \sin\alpha E_y e^{j\Delta\gamma}, \quad (5)$$

where $\Delta\gamma$ in (5) is the static phase difference between E_x and E_y introduced by PC before polarizer. When the combined electrical fields in two paths are sent to the low-speed photodetectors (PDs), the output photocurrents in two paths can be both expressed as

$$\begin{aligned} I(t) \propto R \cdot Y[&\cos^2\alpha \cos(\omega_F t + \theta) - \sin^2\alpha \cos(\omega_F t + \theta) \\ &- \cos\alpha \sin\alpha \cos(\omega_F t - \Delta\gamma + \theta) + \cos\alpha \sin\alpha \cos(\omega_F t + \Delta\gamma + \theta)], \end{aligned} \quad (6)$$

where only the IF signal at $\omega_F = \omega_{RF} - \omega_{LO}$ is considered, and $Y = |E_{in}|^2 \cdot J_{01}J_{02}J_{11}J_{02}$, $\theta = \theta_1 - \theta_0$, R is the responsivity of PD. When $\Delta\gamma = \pi/2$, (6) can be derived as

$$i(t) \propto R \cdot Y \cos(\omega_F t + 2\alpha + \theta). \quad (7)$$

From (7), it is clear that an MPS for the IF signal is implemented, similar to that for processing microwave signal in [27]. Accordingly, the in-phase IF signal [i.e., $\cos(\omega_F t + \theta)$] and quadrature IF signal [i.e., $\sin(\omega_F t + \theta)$] can be generated in two paths for $\alpha = 0$ and $\alpha = -45^\circ$, respectively. Afterwards, as the theory of Hartley architecture shown in Fig.1, to implement image rejection, electrical processing of I and Q IF signals is required. An electrical 90-degree hybrid is used to implement real-time analog processing. Moreover, to achieve large IRR, the I and Q IF signals with low frequency are sampled by the ADC and thereby off-line digital processing is carried out.

C. Digital post-processing for image rejection

In practical applications, the imbalances of gain and phase are inherently existed for different physical path and devices in two I and Q paths. Therefore, by ignoring the constant term (i.e., θ) in (7), the detected I and Q IF signals can be expressed as

$$I_{IF}(t) = G_1 \cos(\omega_{RF} t - \omega_{LO} t), \quad (8)$$

$$Q_{IF}(t) = G_2 \sin(\omega_{RF} t - \omega_{LO} t - \Delta\theta), \quad (9)$$

where G_1 and G_2 represent the amplitudes of the I and Q IF signals, and $\Delta\theta$ is the phase deviation for accurate 90 degree phase shift. Here, we assume the frequency of target signal as $\omega_{RF} = \omega_{LO} + \omega_{IF}$ and that of image signal as $\omega_{RF} = \omega_{LO} - \omega_{IF}$. For the image signal, the I and Q IF signals can be rewritten as

$$I_{IF}(t) = G_1 \cos(\omega_{IF} t), \quad (10)$$

$$Q_{IF}(t) = -G_2 \sin(\omega_{IF} t + \Delta\theta). \quad (11)$$

The amplitude imbalance can be easily compensated by comparing the maximum values of fast Fourier transform (FFT) power spectra of two I and Q IF signals. To compensate the phase imbalance, we multiply the FFT of quadrature IF signal by the coefficient of $\exp(j*(\pi/2 - \Delta\theta)*\mathrm{sgn}(\omega))$, and

$$\mathrm{sgn}(\omega) = \begin{cases} 1 & \omega > 0 \\ -1 & \omega < 0 \end{cases}. \quad (12)$$

Hence, the phase shift of $\pi/2 - \Delta\theta$ can be achieved in time domain for the quadrature IF signal, which can be described as

$$Q_{IF\_processed}(t) = -G_2 \cdot \beta \cos(\omega_{IF} t). \quad (13)$$

From (13), it is can be easily derived that when $\beta = G_1 / G_2$, the image signal can be totally eliminated by adding the digitally processed quadrature IF signal and unprocessed in-phase IF signal.

While for the target signal at $\omega_{RF} = \omega_{LO} + \omega_{IF}$, the I and Q IF signals is

$$I_{IF}(t) = G_1 \cos(\omega_{IF} t), \quad (14)$$

$$Q_{IF}(t) = G_2 \sin(\omega_{IF} t - \Delta\theta). \quad (15)$$

Then, after digital processing, the phase-shifted quadrature IF signal is $G_2 \cdot \beta \cos(\omega_{IF} t - 2\Delta\theta)$. Therefore, the target signal can be optically down-converted to the IF signal, while the image signal is suppressed after digital processing. It should be noticed that, in the digital post-processing, the value of $\Delta\theta$ is obtained by searching the optimum value to achieve a maximum IRR within a certain phase range. Accordingly, to reduce the time and space complexity of digital signal processing (DSP), photonic generation of accurate I and Q IF signals is highly required in the proposed approach.

III. Experiments and Discussion

To verify the proposed approach, experiments based on the setup shown in Fig. 2(a) are performed. The optical carrier with power of 11 dBm is emitted from a tunable narrow linewidth laser with wavelength at 1551.18 nm. The lightwave is then

This article has been accepted for publication in a future issue of this journal, but has not been fully edited. Content may change prior to final publication. Citation information: DOI 10.1109/JQE.2017.2704929, IEEE Journal of Quantum Electronics

modulated by RF signal using a PM with 3-dB bandwidth of 40 GHz and half-wave voltage of 7 V. Another 40-GHz PolM with a half-wave voltage of 5.3 V is connected to the PM via a 2-km single-mode fiber (SMF) spool and driven by the LO signal. An OBPF is used to filter out one of the first-order sideband and the EDFA is used to amplify the optical signal. Afterwards, the amplified signal is split into two paths and each path contains a PC and a polarizer. By adjusting PC2 and PC3, the optical signals in two paths are then applied to the low-speed PDs for the generation of I and Q IF signals. Eventually, the generated I and Q IF signals are sent to the electrical processing module for image rejection.

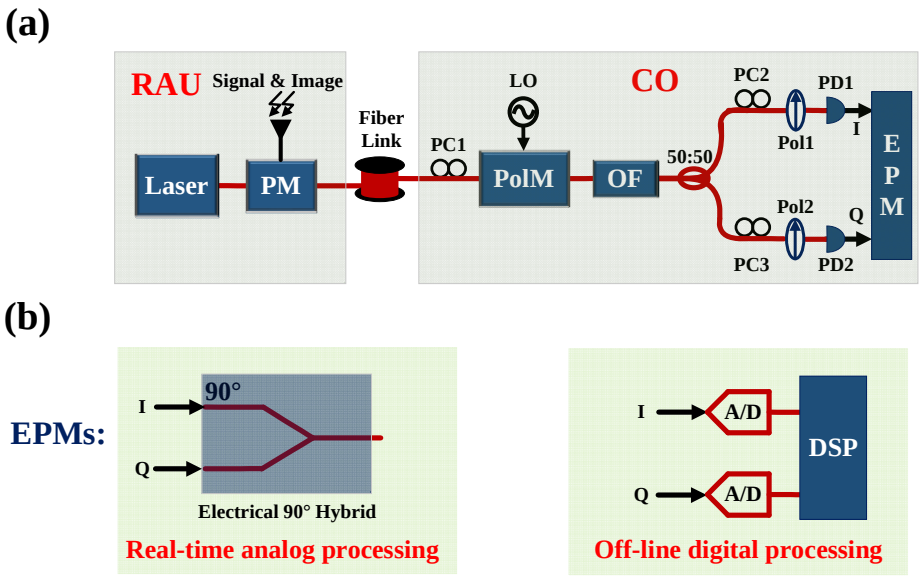

Fig.2. (a) Schematic of the proposed photonics-assisted microwave frequency down-conversion approach. PM: phase modulator, PC: polarization controller; PolM: polarization modulator; OF: optical bandpass filter; Pol: polarizer; EDFA: Erbium-doped fiber amplifier; OC: optical coupler; PD: photodetector; EPM: electrical processing module. RAU: remote antenna unit; CO: central office. (b) Real-time analog and off-line digital EPMs. A/D: analog-to-digital conversion; DSP: digital signal processing;

The target sinusoidal signal at 35.5 GHz generated from a microwave signal generator is firstly applied to the PM. A 35-GHz microwave LO signal is applied to the PolM. The power levels of the target sinusoidal RF and LO signals are set as 10 dBm and 11 dBm, respectively, to optimize the conversion efficiency of the proposed MPM. Figure 3 shows the optical spectra before and after OF. Noted that, in theory, a carrier-suppressed single-sideband (CS-SSB) modulation is still available for the generation of I and Q IF signals and the unwanted mixing spurs can be eliminated as in [20]. However, to cover lower frequency range, SSB modulation is used here for the limited roll-off factor of OBPF. As shown in Fig. 3, the upper sidebands are effectively suppressed by the OBPF while the optical carrier and lower sidebands are remained with few power losses.

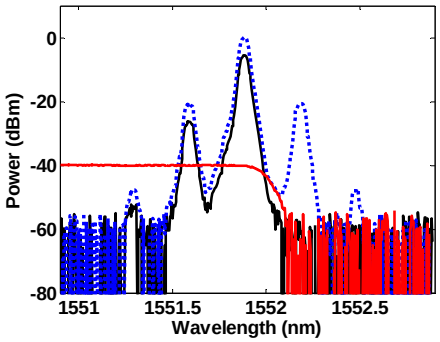

Fig.3. Measured optical spectra before (blue dashed line) and after (black line) OBPF; red line: spectral response of OBPF.

A. Real-time analog processing of I and Q IF signals

First, the optical powers injected into the two PDs of identical responsivity are set as 0 dBm. Fig. 4(a) shows the measured electrical waveforms of 0.5-GHz I and Q IF signals, where the photonic generation of accurate I and Q IF signals can be observed. On the other hand, another sinusoidal signal at 34.5 GHz is applied to the PM, acting as an image one. As shown in Fig. 4(b), both the I and Q IF signals are generated, while the quadrature IF signal is shifted by 180° compared with that down-converted from the target signal. It should be emphasized that a built-in integrated polarizer can be found at the input port of the PolM used, whose principle axis is oriented at an angle of 45° with respect to one principle axis of the PolM. Therefore, the adjustment of PC1 is used to maximum the output power of the PolM. Furthermore, in theory, a 90-degree relative phase difference between the I and Q paths is required. Accordingly, in practical experiments, the generation of I and Q IF signals is simply achieved by the adjusting one of the two PCs (PC2 and PC3) in two paths.

When the real-time analog processing method is employed, the I and Q IF signals are combined by using an electrical 90-degree hybrid to implement image rejection, as shown in Fig. 2(b). The corresponding electrical spectra of the IF signals are measured and shown in Fig. 5(a). When the target sinusoidal signal at 35.5 GHz is applied, a 0.5-GHz IF signal

This article has been accepted for publication in a future issue of this journal, but has not been fully edited. Content may change prior to final publication. Citation information: DOI 10.1109/JQE.2017.2704929, IEEE Journal of Quantum Electronics

with a power level of -15 dBm is generated and the IF signal down-converted from the image signal at 34.5 GHz is about -60 dBm, demonstrating an IRR of 45 dB.

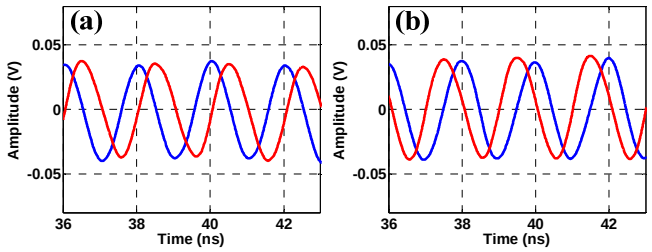

Fig.4. (a) Measured temporal waveforms of I (blue line) and Q (red line) 500-MHz IF signals down-converted from the target signal (a) and image signal (b).

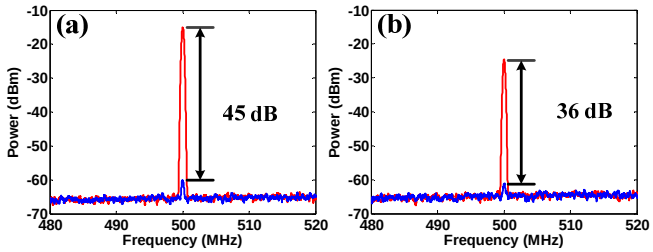

Fig.5. Measured electrical spectra of IF signals down-converted from the target signal (red line) and image signal (blue line) with a (a) 2-km or (b) 25-km fiber link.

Furthermore, to demonstrate the capability of achieving antenna remoting, a 25-km-long SMF is used to replace the 2-km one. As shown in Fig. 5(b), due to the linear transmission loss, the power level of generated IF signal from the target signal decreases to -24.5 dBm. In this way, the measured IRR is 36 dB. However, it should be noticed that the degradation of IRR is mainly due to the reduced peak power of the generated IF signal from target signal, while the IF signal generated from the image signal can be effectively suppressed after transmission over a long fiber link. The phase noises of the generated IF sinusoidal signals for the 2-km and 25-km fiber links are also measured and shown in Fig. 6, where similar phase noise characteristics for two cases are observed.

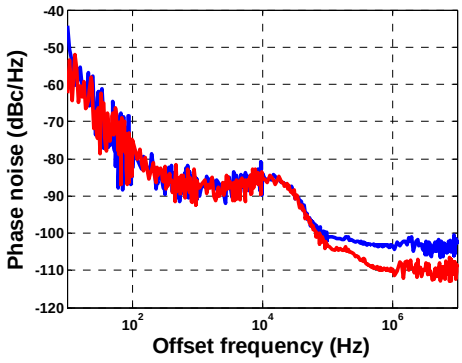

Fig.6. Measured phase noises of the generated IF signals for the 2-km fiber link (red line) and 25-km fiber link (blue line).

With a 2-km fiber link, the conversion efficiency, which is defined as the ratio between output IF power to the RF input power, of proposed down-converter for different RF frequencies in the frequency range from 5 to 40 GHz are measured and shown in Fig.7, where the LO frequency is tuned to obtain 500 MHz IF signals. From Fig. 7, to achieve SSB modulation, the IF output power for RF signal at low frequency will be affected by the limited roll-off factor of OBPF.

Finally, the spurious free dynamic range (SFDR) of the proposed MPM is measured by applying two RF tones at 35.5 and 35.51 GHz. When the frequency of the LO signal is set as 35 GHz, the fundamental harmonic (@ 0.5 or 0.51 GHz) and third-order inter-modulation distortion (IMD3) (@ 0.49 or 0.52 GHz) of the IF signal are measured under different input RF power levels. As illustrated in Fig. 8, the noise floor is measured as -141 dBm in a 300-Hz bandwidth that is limited by the minimum scanning bandwidth of the available electrical spectrum analyzer. Therefore, the calculated SFDR here is calculated as 103 dB·Hz$^{2/3}$. In addition, in our proposal the CS-SSB modulation is still available for the generation of I and Q IF signals. With aid of the CS-SSB modulation, the unwanted mixing spurs can be effectively suppressed and hence the SFDR can be greatly improved [22].

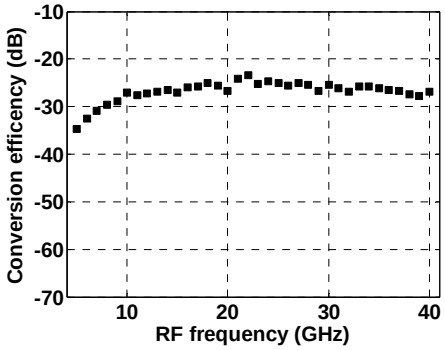

Fig.7. Measured conversion efficiencies for different RF frequencies in the frequency span of 5 to 40 GHz.

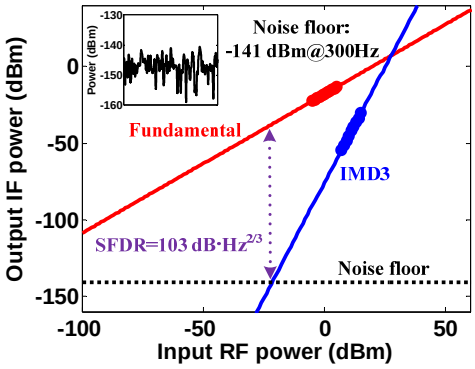

Fig.8. Fundamental harmonic (red line) and third-order distortion (blue line) of the output IF signal measured under different input RF power levels. Inset: measured noise floor in 300-Hz bandwidth (black line).

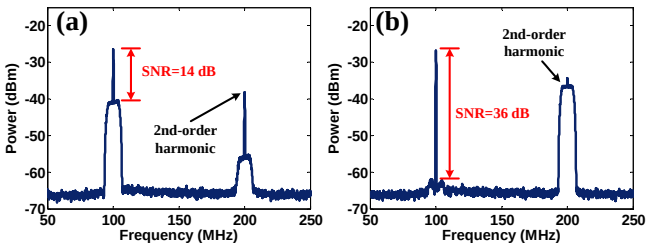

Fig.9. Measured electrical spectra of IF signals processed by the normal electrical 3-dB coupler (a) and electrical 90-degree hybrid (b).

To further verify the image rejection function of the

This article has been accepted for publication in a future issue of this journal, but has not been fully edited. Content may change prior to final publication. Citation information: DOI 10.1109/JQE.2017.2704929, IEEE Journal of Quantum Electronics

proposed approach, we apply a broadband 10-MBaud 16-quadrature-amplitude-modulation (QAM) RF signal at 2.9 GHz generated from a commercial vector signal generator (R&S SMBV100A) and a target sinusoidal RF signal at 3.1 GHz to the PM simultaneously. Another LO signal at 3 GHz is sent to the PolM. Therefore, 100-MHz IF signals with and without the base-band digital signal modulation can be generated by optical mixing. As the measured electrical spectrum shown in Fig. 9(a), when the I and Q IF signals are combined by a normal electrical 3-dB coupler, the IF signal at 100 MHz from the image signal will cause serious distortion to that from the target signal. As shown in Fig. 9(b), after being processed by the electrical 90-degree hybrid, the IF signal from the image signal can be effectively suppressed and the IF signal from the target signal remains, demonstrating an signal-to-noise (SNR) performance improvement of 22 dB. Octave harmonic components such as the 2nd-order one can be eliminated by additional filtering.

B. Off-line digital processing of I and Q IF signals

To implement image rejection with large IRR, the off-line digital processing is carried out to accurately compensate the amplitude and phase imbalances between two generated I and Q IF signals. To simulate the amplitude imbalance, two PDs with different responsivities are used and the generated electrical signals in two paths are digitalized by two channels of real-time oscilloscope running at 40 GS/s (LeCroy WaveMaster 813Zi-A) for the digital post-processing. The data length and time window are set to be 200002 and 5 μs respectively, to recover the signal without distortion.

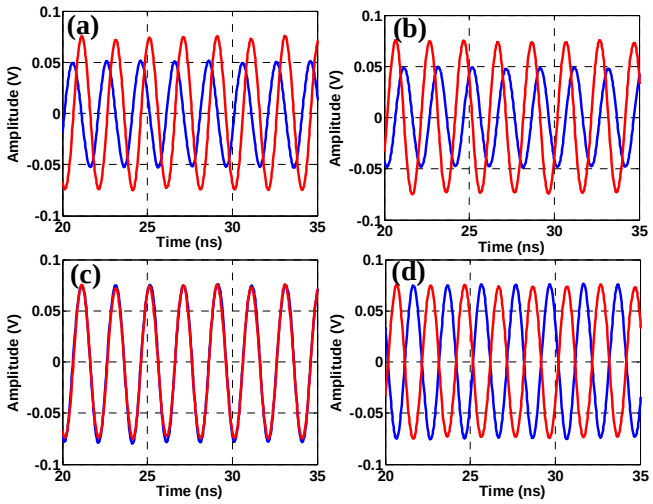

Fig.10. Measured temporal waveforms of I (red line) and Q (blue line) 500-MHz IF signals down-converted from the target (a) and image (b) signals; Temporal waveforms of I (red line) and Q (blue line) IF signals after DSP compensation for that down-converted from the target (c) and image (d) signals.

For the case of sinusoidal image signal at 34.5 GHz, Fig. 10(a) and (b) shows the measured electrical waveforms of I and Q IF signals at 500 MHz for the target and image signals. Obviously, the RF signal at 35.5 GHz is successfully down-converted to the IF signal at 500 MHz and photonic generation of accurate I and Q IF signals can be observed. However, as shown in Fig. 10(a), two I and Q IF signals suffer from the amplitude imbalance for different devices used in two paths. In addition, due to the environment induced state of polarization (SOP) change, 1°~3° phase fluctuations for I and Q IF signals are observed by the real-time oscilloscope. These imbalances of amplitude and phase will have serious impact on the IRR.

To achieve large IRR, digital post-processing technology is used to compensate the amplitude and phase imbalances between the I and Q IF signals. Figure. 10(c) and (d) shows the temporal waveforms of I and Q IF signals after digital processing for imbalances compensation, where we can find that amplitudes of two I and Q IF signals at 500 MHz are nearly the same. Two I and Q IF signals are out-of-phase for the image signal and in-phase for the target signal. Therefore, by adding two I and Q IF signals, the IF signal at 500 MHz down-converted from image signal can be effectively suppressed and that from the target signal remains.

As seen in Figs.11(a) and (b), after DSP processing, the IF signal down-converted from the image signal is suppressed to below the noise level, while that down-converted from the target signal is maintained, indicating an IRR beyond 60 dB. Furthermore, since the advanced digital post processing method can accurately compensate the amplitude and phase imbalances in two signal paths, we believe the IRR is only limited by the processing resolution of ADC and signal-to-noise ratio of received IF signal.

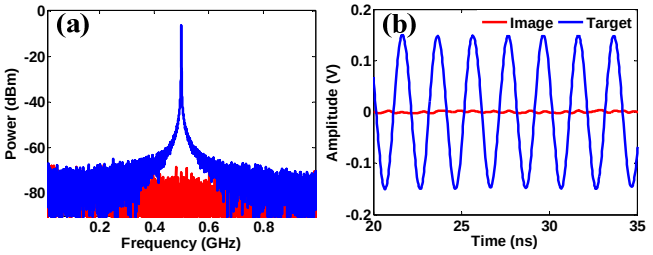

Fig.11. (a) FFT power spectra of IF signals down-converted from the target signal (blue line) and image signal (red line) after DSP processing. (b) Temporal waveforms of IF signals down-converted from the target signal (blue line) and image signal (red line) after DSP processing.

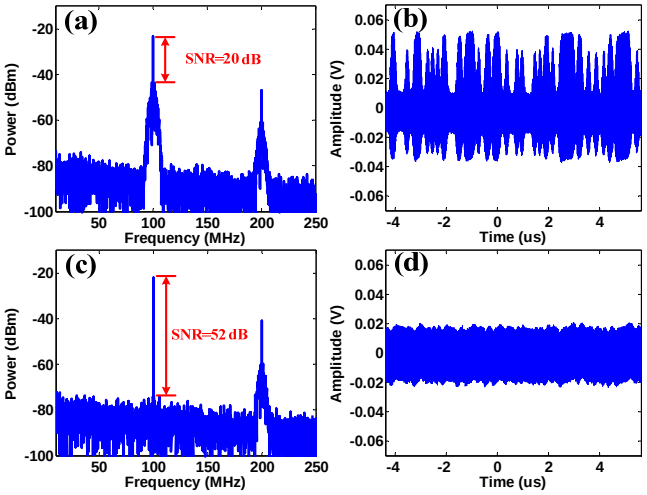

Fig.12. FFT power spectra (a) before and after (c) DSP compensation; temporal waveforms (b) before and (d) after DSP compensation.

For the case of broadband image RF signal at 2.9 GHz, carrying 10-Mbit/s on-off keying (OOK) data, Figs. 12(a) and (b) demonstrate the FFT power spectrum and temporal

waveform of the IF signal at the in-phase path, in which we can find that the IF signal at 100 MHz from the image signal will cause serious distortion to that from the target signal without DSP. While as shown in Figs. 12(c) and (d), after DSP compensation, the IF signal from the image signal can be effectively suppressed and the IF signal from the target signal remains. With the DSP, a 32-dB improvement for the SNR performance is observed.

In addition to the suppression of image signal, the overall link linearity can also be improved by using digital post-processing technology, such as the results released in [11]-[14].

IV. Conclusion

A photonic approach was proposed to perform microwave frequency down-conversion with a high IRR for antenna remoting. I and Q IF signals were first generated by using cascaded electro-optic modulators and then the digital post-processing method was used to compensate for the amplitude and phase imbalances between the I and Q IF signals. In the proof-of-concept experiments, transmissions of RF signals over the fiber links of 2 km and 25 km are implemented. The real-time analog and off-line digital processing methods were used to process the I and Q IF signals for image rejection, when adding two different types of image signals. Concerning a sinusoidal image signal, an IRR over 45 dB was achieved using the real-time analog method; with the assistance of the off-line digital method, an IRR beyond 60 dB was obtained. The distortions from a broadband image RF signal carrying baseband signal were also effectively suppressed by using one of the two processing methods. Due to the wide bandwidth of the optical components used in the mixing structure, the proposed microwave frequency down-conversion approach can operate within a wide RF frequency range from 5 to 40 GHz.

References

[1] W. S. C. Chang, *RF Photonic Technology in Optical Fiber Links*, 1sted. Cambridge, U.K.: Cambridge Univ. Press, 2002.

[2] J. P. Yao, "Microwave photonics," *J. Lightw. Technol*., vol. 27, no. 3, pp.314-335, Feb. 2009.

[3] M. Li, et al., "Reconfigurable single-shot incoherent optical signal processing system for chirped microwave signal compression," *Sci. Bull.*, vol. 62, no. 4, pp. 242-248, Jan. 2017.

[4] Z. Cao, X. Zhao, F. M. Soares, N. Tessema, and A. M. J. Koonen, "38-GHz millimeter wave beam steered fiber wireless systems for 5G indoor coverage: architectures, devices, and links," *IEEE J. Quantum Electron.*, vol. 53, no. 2, Feb. 2017, Art. no. 8000109.

[5] G. K. Gopalakrishnan, W. K. Burns, and C. H. Bulmer, "Microwave-optical mixing in Limo3 modulators," *IEEE Trans. Microw. Theory Tech*., vol. 41, no. 12, pp. 2383-2391, Dec. 1993.

[6] C. K. Sun, R. J. Orazi, S. A. Pappert, and W. K. Bums, "A photonic-link millimeter-wave mixer using cascaded optical modulators and harmonic carrier generation," *IEEE Photon. Technol. Lett*., vol. 8, no. 9, pp. 1166-1168, Sep. 1996.

[7] E. H. W. Chan and R. A. Minasian, "Microwave photonic downconverter with high conversion efficiency," *J. Lightw. Technol*., vol. 30, no. 23, pp. 3580-3585, Dec. 2012.

[8] E. H. W. Chan and R. A. Minasian, "High conversion efficiency microwave photonicmixer based on stimulated Brillouin scattering carrier suppression technique," *Opt. Lett*., vol. 38, no. 24, pp. 5292-5295, Dec. 2013.

[9] A. Karim and J. Devenport, "High dynamic range microwave photonic links for RF signal transport and RF-IF conversion," *J. Lightw. Technol.*, vol. 26, no. 15, pp. 2718‑2724, Aug. 2008.

[10] V. R. Pagan, B. M. Haas, and T. E. Murphy, "Linearized electrooptic microwave down-conversion using phase modulation and optical filtering," *Opt. Express*, vol. 19, no. 2, pp. 883-895, Jan. 2011.

[11] A. Altaqui, E. H. W. Chan, and R. A. Minasian,. "Microwave photonic mixer with high spurious-free dynamic range," *Applied Optics*, vol. 53, no. 17, pp. 3687-3695, 2014.

[12] T. Jiang, S. Yu, C. Luo and J. Li, "Digital linearization and full spectrum utilization for phase-modulation photonic down-conversion", *IEEE Photon. Technol. Lett.*, vol. 25, no. 20, pp. 2010-2013, Sep. 2013.

[13] T. R. Clark, S. R. O' Connor, and M. L. Dennis, "A phase-modulation I/Q-demodulation microwave-to-digital photonic link," *IEEE Trans. Microw. Theory Tech*., vol. 58, no. 11, pp. 3039‑3058, Nov. 2010.

[14] L. Huang, et al., "Photonic down-conversion of RF signals with improved conversion efficiency and SFDR," *IEEE Photon. Technol. Lett*., vol. 28, no. 8, pp. 880-883, Apri. 2016.

[15] Y. Pan, et al., "Adaptive linearized microwave down-conversion utilizing a single dual-electrode Mach–Zehnder modulator," *Opt. Lett*., vol. 40, no. 11, pp. 2649-2652, Jun. 2015.

[16] D. Zou, X. P. Zheng, S. Y. Li, H. Zhang, and B. K. Zhou, "Idler-free microwave photonic mixer integrated with a widely tunable and highly selective microwave photonic filter," *Opt. Lett*., vol. 19, no. 13, pp. 3954-3957, 2014.

[17] S. J. Strutz and K. J. Williams, "A 0.8-8.8-GHz image rejection microwave photonic downconverter," *IEEE Photon. Technol. Lett.*, vol. 12, no. 10, pp. 1376-1378, Oct. 2000.

[18] S. Wu and B. Razavi, "A 900-MHz/1.8-GHz CMOS Receiver for Dual-Band Applications," *IEEE J. Solid-State Circuits*, vol. 33, no. 12, pp. 2178–2185, Dec. 1998.

[19] L. Chao, C. Wenyue, and J. F. Shiang, "Photonic mixers and image-rejection mixers for optical SCM systems," *IEEE Trans. Microw. Theory Tech.*, vol. 45, no.8, pp. 1478-1480, Aug. 1997.

[20] S. L. Pan and Z. Z. Tang, "A highly reconfigurable photonic microwave frequency mixer," SPIE Nesroom, DOI: 10.1117/2.1201501.005736, Feb. 2015.

[21] Z. Z. Tang, and S. L. Pan, "Image-reject mixer with large suppression of mixing spurs based on a photonic microwave phase shifter," *J. Lightw. Technol*., vol. 34, no. 20, pp. 4729-4735, Oct. 2016.

[22] Z. Z. Tang, and S. L. Pan, "A reconfigurable photonic microwave mixer using a 90° optical hybrid," *IEEE Trans. Microw. Theory Tech*., vol. 64, no. 9, pp. 3017-3025, Sep. 2016.

[23] Zhang, J., et al. "High conversion efficiency photonic microwave mixer with image rejection capability." *IEEE Photon. J.* vol. 8, no. 4, 1-11, Aug. 2016.

[24] C. Liu, et al., "A novel multi-service small-cell cloud radio access network for mobile backhaul and computing based on radio-over-fiber technologies," *J. Lightw. Technol*., vol. 31, no. 17, pp. 2860-2857, Sep. 2013.

[25] V. R. Pagán and T. E. Murphy, "Electro-optic millimeter-wave harmonic downconversion and vector demodulation using cascaded phase modulation and optical filtering," Opt. Lett., vol. 40, no. 11, pp. 2481-2484, Jun. 2015.

[26] P. Li, X. Zou, W. Pan, and L. Yan, "Microwave photonic down-conversion with large image rejection ratio utilizing digital signal processing," in Proc. the Asia Communication Photonics Conf., Wuhan, China, 2016, Paper ATh3H.3.

[27] S. L. Pan and Y. M. Zhang, "Tunable and wideband microwave photonic phase shifter based on a single-sideband polarization modulator and a polarizer," Opt. Lett. vol. 37, no. 21, pp. 4483-4485, Nov. 2012.

Peixuan Li received the BS degree from Southwest Jiatotong University, China, in 2012. He is currently working toward the Ph.D. degree in the School of Information Science and Technology, Southwest Jiaotong University. His current research interests include microwave photonic processing and generation, fiber communication systems.

Wei Pan is a currently Full Professor and the Dean of the School of Information Science and Technology, Southwest Jiaotong University, China. His research interests include semiconductor lasers, nonlinear dynamic systems,

This article has been accepted for publication in a future issue of this journal, but has not been fully edited. Content may change prior to final publication. Citation information: DOI 10.1109/JQE.2017.2704929, IEEE Journal of Quantum Electronics

and optical communications. He has published over 200 papers in high-impact refereed journals.

Dr. Pan was appointed as the steering and consultancy expert of the highest level national project (973 Project) of China. He was also awarded as the Academic and Technology Leader of Sichuan province, China.

Xihua Zou is currently a Full Professor in the Center for Information Photonics & Communications, Southwest Jiaotong University, China. Since October 2014, he has been working as a Humboldt Research Fellow in the Institute of Optoelectronics, University of Duisburg-Essen, Germany. He once was a visiting researcher and a joint training Ph.D. student in the Microwave Photonics Research Laboratory, University of Ottawa, Canada, in July and August of 2011 and in 2007-2008, respectively. He was also a visiting scholar in the Ultrafast Optical Processing Research Group, INRS-EMT, Canada, in July and August of 2012. His current interests include microwave photonics, radio over fiber, and optical communications. He has authored or coauthored over 80 academic papers in high-impact refereed journals.

Dr. Zou was a recipient of the Alexander von Humboldt Research Fellowship, National Outstanding Expert in Science & Technology of China, the Nomination Award for the National Excellent Doctoral Dissertation of China, the Science & Technology Award for Young Scientist of Sichuan Province, China, and the Outstanding Reviewer of Optics Communications. He currently serves as an Associate Editor of IEEE Journal of Quantum Electronics, the Guest Editor for a Special Section on Microwave Photonics in IEEE/OSA Journal of Lightwave Technology, and once as the Editor and the Coordinator for a Focus Issue on Microwave Photonics in IEEE Journal of Quantum Electronics, and the leading Guest Editor for a Special Section on Microwave Photonics in Optical Engineering.

Bing Lu was born in Henan, China, in 1986. He received the B.S. degree in Zhoukou Normal University, Zhoukou, China, in 2010. He is currently working toward the Ph.D. degree in the School of Information Science and Technology, Southwest Jiaotong University, China. His research interests include the microwave photonics and optical communication.

Lianshan Yan is currently a Full Professor and the Director of Center for Information Photonics and Communications in Southwest Jiaotong University, China.

Dr. Yan received the IEEE Photonics Society Distinguished Lecturer Award for 2011-2013 and the IEEE LEOS Graduate Fellowship in 2002. He currently serves as the Chair of the Fiber Optics Technology Technical Group, the Optical Society of America (OSA). He served as the co-chair or the TPC member of more than 20 international conferences, including the Optical Fiber Communication Conference and Exposition (OFC, 2013-), the European Conference on Optical Communication (ECOC, 2013-), the Asia Communications and Photonics Conference (ACP, 2010-2012), etc. He once served as an Associate Editor of *IEEE Photonics Journal*.

Bin Luo received the Ph.D. degree from Southwest Jiaotong University, Chengdu, China, in 1995. He is currently a Professor with the School of Information Science and Technology, Southwest Jiaotong University. He is the author or coauthor of more than 80 research papers. His current research interests include semiconductor optical amplifiers and optical communication.